

# Self-localization of a single hole in Mott antiferromagnets

Zheng Zhu<sup>1</sup>, Hong-Chen Jiang<sup>2,3</sup>, Yang Qi<sup>1</sup>, Chu-Shun Tian<sup>1</sup>, and Zheng-Yu Weng<sup>1</sup>

<sup>1</sup>*Institute for Advanced Study, Tsinghua University, Beijing, 100084, P. R. China*

<sup>2</sup>*Kavli Institute for Theoretical Physics, University of California,*

*Santa Barbara, CA, 93106-4030, U.S.A.*

<sup>3</sup>*Center for Quantum Information, IIS,*

*Tsinghua University, Beijing, 100084, China*

(Dated: September 20, 2018)

## Abstract

A long-standing issue<sup>1-15</sup> in the physics of strongly correlated electronic systems is whether the motion of a single hole in quantum antiferromagnets can be understood in terms of the quasiparticle picture. Very recently, investigations of this issue have been within the experimental reach<sup>16</sup>. Here we perform a large-scale density matrix renormalization group study, and provide the first unambiguous numerical evidence showing that in ladder systems, a single hole doped in the Mott antiferromagnet does not behave as a quasiparticle. Specifically, the injected hole is found to be always localized as long as the leg number is larger than one, with a vanishing quasiparticle weight and a localization length monotonically decreasing with the leg number. In addition, the single hole self-localization is insensitive to the parity (even-odd) of the leg number. Our findings may advance conceptual developments in different fields of condensed matter physics. First of all, the intriguing self-localization phenomenon is of pure strong correlation origin free of extrinsic disorders. Therefore, it is in sharp contrast to the well-known Anderson localization<sup>17</sup> and recently found many-body localization<sup>18</sup>, where extrinsic disordered potentials play crucial roles. Second, they confirm the analytical predictions<sup>14,15</sup> of the so-called phase string theory<sup>13,14</sup>, suggesting that the phase string effect lies in the core of the physics of doped Mott antiferromagnets.

The doped Mott insulator is generally believed to be the prototypical model of many realistic strongly correlated systems notably high  $T_c$  cuprates<sup>1,19,20</sup>, and is a fundamental problem of great challenge in condensed matter physics. Important insights into doped Mott insulators may be gained by inspecting a special case namely the single hole doped Mott insulator. This has been under intense investigations<sup>1-15</sup> for over decades, but remained highly controversial. On the one hand, a quasiparticle weight was found by using either analytic approaches (in combination with the self-consistent Born approximation)<sup>4-7</sup> or finite-size exact diagonalization<sup>8</sup> on lattices up to 32 sites<sup>9</sup>. This indicates that an injected hole with a Fermi momentum maintains coherent motion in the quantum antiferromagnetic spin background. On the other hand, the validity of such a quasiparticle picture has been seriously questioned<sup>2,12-15</sup> by various authors. It was first argued by Anderson<sup>2</sup> that the quasiparticle weight vanishes when a hole is injected into the Mott insulator. Later, this crucial observation received justification on a completely microscopic level: by identifying the so-called phase string effect<sup>13,14</sup>, it was proved that the quasiparticle weight indeed vanishes at the ground states. In addition, it was further predicted<sup>15</sup> that the non-perturbative phase string effect may lead to self-localization of the injected hole.

On the experimental side, in earlier angle-resolved photoemission spectroscopy (ARPES) studies<sup>21-23</sup>, broad spectral features have been observed in materials such as  $\text{Ca}_2\text{CuO}_2\text{Cl}_2$  and  $\text{Sr}_2\text{CuO}_2\text{Cl}_2$ . This shows indirectly that the motion of a single hole in quantum antiferromagnets may not be understood in terms of the quasiparticle picture<sup>15,23</sup>. Very recently, an unprecedented degree of control has been reached in experiments with the  $\text{Ca}_2\text{CuO}_2\text{Cl}_2$  parent Mott insulators, opening a new route for experimental study of a single charge doped Mott insulator. In particular, scanning tunneling microscope (STM) experiments on the atomic scale electronic structure of this material have unveiled a striking phenomenon: a single electron donated by surface defect creates an electronic state strongly localized in space<sup>16</sup>. Consistent with the earlier ARPES experiments above, the observed localization of the single doped charge also does not support the quasiparticle picture.

While numerical simulation serves as a powerful tool for resolving this puzzle, a crucial point is how to extend results obtained from finite-size numerical simulations to the large sample limit. To the best of our knowledge, this issue has not yet been addressed in the literature. The purpose of this work is to carry out the first large-scale numerical study and resolve the important issue of the validity of the quasiparticle picture in lightly doped Mott

antiferromagnets.

To this end, we adopt the unbiased density matrix renormalization group (DMRG) method<sup>24</sup> to extensively investigate this problem in ladder systems. We find that if a ladder sample is sufficiently long, the injected hole is always localized in the quantum antiferromagnetic spin background, once the leg number is larger than one. In fact, the localization length gets continuously reduced with the increase of the leg number, pointing to a strong localization in the two-dimensional limit. Contrary to this, if the sample is sufficiently short, the injected hole remains itinerant. This suggests that quasiparticle behavior found in earlier numerical study<sup>8,9</sup> is likely a small-size effect. The intriguing phenomenon of self-localization of a single hole in Mott antiferromagnets and the vanishing quasiparticle spectral weight in the large sample limit constitute the unambiguous numerical evidence showing that a single hole doped into the Mott antiferromagnet no longer behaves like a quasiparticle. These support the analytic predictions<sup>14,15</sup> of the phase string theory for doped quantum antiferromagnets.

*Model and numerical method.*— The DMRG calculation is performed for the  $t$ - $J$  model Hamiltonian,

$$H_{tJ} = -t \sum_{\langle ij \rangle \sigma} (c_{i\sigma}^\dagger c_{j\sigma} + h.c.) + J \sum_{\langle ij \rangle} (\mathbf{S}_i \cdot \mathbf{S}_j - \frac{1}{4} n_i n_j). \quad (1)$$

Here,  $c_{i\sigma}^\dagger$  is the electron creation operator at site  $i$ ,  $\mathbf{S}_i$  the spin operator, and  $n_i$  the number operator. The summation is over all the nearest-neighbors,  $\langle ij \rangle$ . The Hilbert space is constrained by the no-double-occupancy condition, i.e.,  $n_i \leq 1$ . At half-filling,  $n_i = 1$ , the system reduces to Mott insulators (antiferromagnets) with a superexchange coupling,  $J$ . Upon doping a hole into this system,  $\sum_i n_i = N - 1$  ( $N$  the number of the lattice sites), and the hopping process is triggered as described by the first term of equation (1), with  $t$  the hopping integral.

Below, we shall focus on bipartite lattices of  $N = N_x \times N_y$ , where  $N_x$  and  $N_y$  are the numbers of sites along the  $x$  and  $y$  directions, respectively. We shall study the ladders with a finite  $N_y$  (from 1 to 5) and sufficiently large  $N_x$ . We set  $J = 1$  as the unit of energy and focus on the  $t/J = 3$  case unless otherwise specifically stated. For the numerical simulation, we use fully open boundary conditions, and keep enough number of states in each DMRG block. Excellent convergence is achieved with total truncation error of the order of  $\leq 10^{-7}$ .

*Self-localization of the doped hole.*— One of the main findings of the present work is that

the single hole is found to be localized for the leg number  $N_y > 1$ . Examples of the hole density distribution,  $\langle n_i^h \rangle \equiv 1 - \langle n_i \rangle$ , are shown in Fig. 1 (a) and (b) for  $N_y = 3$  and 4, respectively, where the sample size  $N_x = 200$  is clearly much larger than the localization lengths. In Fig. 1 (a) and (b), we plot the hole density at a middle leg of the ladders along the  $x$  direction. We have checked that upon summing up the distribution from different legs, the sum rule  $\sum_i \langle n_i^h \rangle = 1$  is satisfied. Examples of the contour plot of  $\langle n_i^h \rangle$  in the  $x$ - $y$  plane can be found in Supplementary Information.

To determine the localization length, we note that each density profile is well fitted by a Gaussian distribution function. Then, the localization length is defined as the full width at half-maximum (FWHM) of the distribution. If the doped hole is itinerant, the FWHM should increase monotonically with the sample length ( $N_x$ ); in contrast, if the doped hole is localized, the FWHM should saturate at certain sample length, with the saturation value giving the localization length. Fig. 1 (c) shows that the FWHM for each of the ladders, from  $N_y = 1$  to 5, increases linearly for small sample lengths, while saturates for sufficiently large sample lengths (except the  $N_y = 1$  case, as shown in the inset of Fig. 1 (c)). These results indicate that the single hole is well localized in space with a Gaussian profile of the density distribution. In particular, Fig. 1 (c) clearly shows that the saturated FWHM at  $N_y > 1$  monotonically decreases with the increase of the leg number  $N_y$ , implying the localization be even stronger in the two-dimensional limit. By contrast, there is no indication of saturation in FWHM for long one-dimensional ( $N_y = 1$ ) chains with  $N_x$  up to 300 (see the inset of Fig. 1 (c)), which is consistent with the fact that the doped hole in one dimensions is known to follow the Luttinger liquid behavior instead of being localized<sup>1,14</sup>.

Figure 1 (a) and (b) show that the hole is localized in the central region of the sample. This is due to the fact that an open boundary condition is used for the DMRG calculation. We also add an artificial local chemical potential  $\mu (= 0.08)$  at the site  $x = 31$ , and find that the hole density profile is moved and peaks at the impurity accordingly (see Fig. 1 (d)). This suggests the robustness of localization.

Although the self-localization of the doped hole is insensitive to the parity (even-odd) of the leg number, as shown in Fig. 1 (a) and (b) as well as in Supplementary Information, the hole distribution function  $\langle n_i^h \rangle$  does clearly exhibit a parity effect: for the even-leg ladders ( $N_y = 2, 4$ ), there are always small site-dependent oscillations on top of the Gaussian density profile of  $\langle n_i^h \rangle$ , while they are absent for the odd-leg ladders ( $N_y = 3, 5$ ). We point out

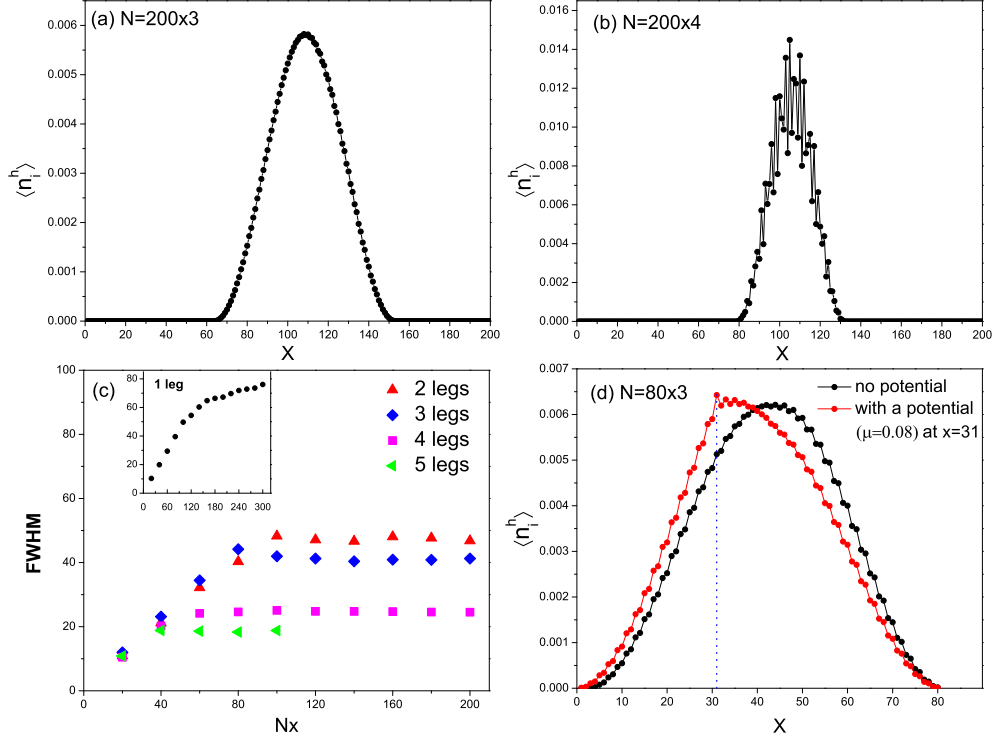


Fig. 1: **Self-localization of the doped hole.** In the 3-leg ladder system of size  $N=200 \times 3$  (a) and 4-leg ladder of  $N=200 \times 4$  (b), single hole doped into the antiferromagnets is well localized as shown by the density distribution  $\langle n_i^h \rangle$  in a middle leg (along the  $x$  axis).  $\langle n_i^h \rangle$  is well fitted by the Gaussian function with the full width at half-maximum (FWHM) defining the localization length. The behavior of the FWHM depends on the width  $N_y$  (c): for the ladders of  $N_y > 1$ , the FWHM first increases linearly at small  $N_x$  and then saturates at large  $N_x$ , with the saturation values much smaller than the maximal  $N_x (= 200)$  and monotonically decreasing with the leg number; for the one-dimensional ( $N_y = 1$ ) chain, the FWHM increases monotonically with the sample length without saturation (the inset of (c)). With the open boundary condition, the hole is naturally localized at the central region of the sample. Nevertheless, it can be easily shuffled by adding a small local chemical potential  $\mu$  as shown in (d) (where  $\mu = 0.08$  at  $x = 31$ ).

that this can be attributed to the underlying distinct spin-spin correlations for the odd- and even-leg ladders at half-filling that follow a power-law (reflecting the absence of spin gap) and exponential (reflecting the presence of spin gap) decay, respectively (see Supplementary Information). In fact, with the increase of the hopping integral  $t$ , the spin-gap effect will be gradually reduced such that the parity effect eventually disappears at large  $t/J$  limit,

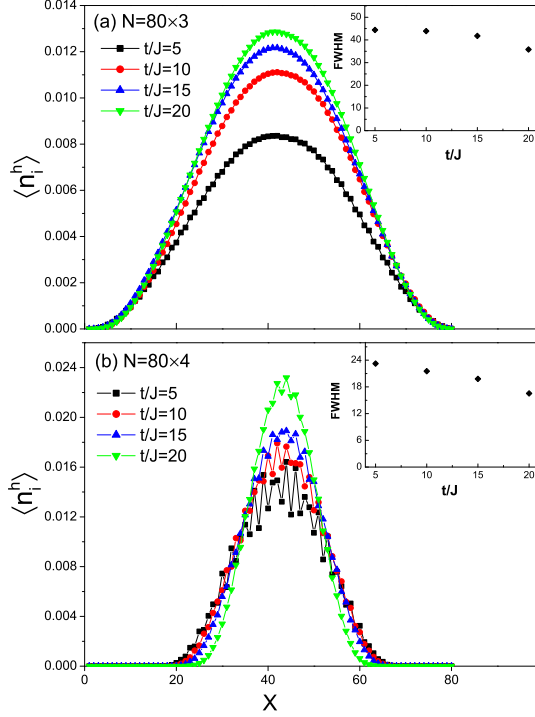


FIG. 2:  $t/J$ -dependence of the hole density distribution. For different  $t/J$  ratios, we plot  $\langle n_i^h \rangle$  at the middle chain along the  $x$  axis for the ladders of size  $N = 80 \times 3$  (a) and  $N = 80 \times 4$  (b). The localization length (the FWHM) is reduced with the increase of  $t/J$  (see the insets). Moreover, the oscillation in the 4-leg ladder system becomes smaller with the increase of  $t/J$ , indicating the convergence of the even- and odd-leg ladders.

where the aforementioned oscillation in  $\langle n_i^h \rangle$  for the even-leg ladders is also diminished as illustrated in Fig. 2 (b). The localization length is actually monotonically reduced as the ratio  $t/J$  increases as shown in the insets of Fig. 2. It thereby suggests that the detailed spin dynamic behavior, governed by the superexchange  $J$ , is not essential to the hole localization.

*Vanishing quasiparticle spectral weight.*—One prominent issue regarding the validity of quasiparticle picture concerns whether the quasiparticle spectral weight  $Z_{\mathbf{k}}$  vanishes at the Fermi momentum. Despite of great efforts<sup>2,4-9,13,14</sup>, this remains highly controversial in the literature. In this part, we turn to study this subject by invoking the state of the art numerical method. The spectral weight  $Z_{\mathbf{k}}$  is defined as

$$Z_{\mathbf{k}} \equiv |\langle \psi_{1-hole} | c_{\mathbf{k}\sigma} | \psi_{0-hole} \rangle|^2, \quad (2)$$

where  $|\psi_{1-hole}\rangle$  is an eigenstate of  $H_{t-J}$  of momentum  $-\mathbf{k}$  in the one hole case,  $|\psi_{0-hole}\rangle$

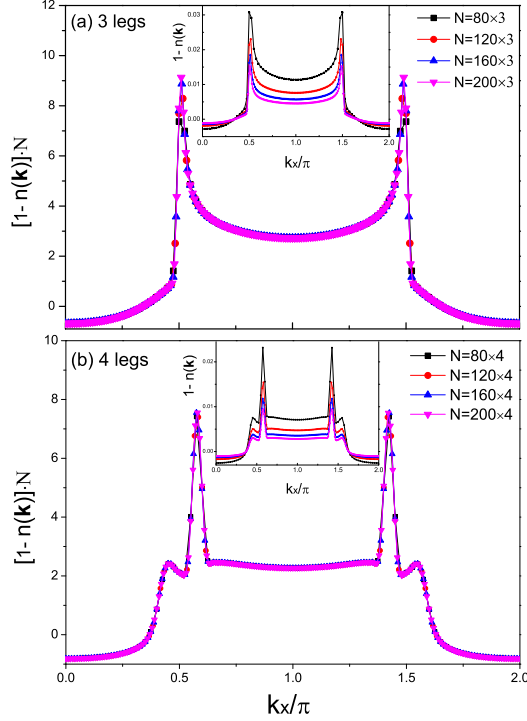


FIG. 3: **Quasiparticle spectral weight.** For both 3-leg (a) and 4-leg (b) ladders, the momentum distribution of the hole exhibits scaling behavior: after the rescaling,  $1 - n(\mathbf{k}) \rightarrow [1 - n(\mathbf{k})]N$ , the curves at different sample lengths in the insets collapse into a single one represented in the corresponding main panels. Note that for the 3-leg case, we fix  $k_y = \frac{2\pi}{3}$  and for the 4-leg case,  $k_y = \frac{\pi}{2}$  and plot the distribution along  $k_x$ . Representative contour plots in the whole  $k_x$ - $k_y$  plane are shown in Supplementary Information.

the ground state at half-filling, and  $c_{\mathbf{k}\sigma}$  is the Fourier transformation of the operator  $c_{i\sigma}$ . Due to the translational symmetry of  $H_{t-J}$ ,  $Z_{\mathbf{k}}$  is well-defined and characterizes the low-lying quasiparticle-like excitations. A finite  $Z_{\mathbf{k}_f}$  means a finite overlap of the bare-hole state  $c_{\mathbf{k}_f\sigma} |\psi_{0-hole}\rangle$  with the true ground state of a single hole at the Fermi momentum  $-\mathbf{k}_f$ . If  $Z_{\mathbf{k}_f} = 0$ , then each injected hole will cause a global adjustment in the ground state, rendering the breakdown of the quasiparticle picture that is perturbatively tractable<sup>1</sup>.

Importantly, the finding of the self-localization of the single hole implies that the doped hole should not behave like a conventional quasiparticle. Consistent with this observation, the quasiparticle spectral weight is numerically found to vanish, as we will show below. Technically, different bases after truncation in the DMRG calculation of  $|\psi_{0-hole}\rangle$  and  $|\psi_{1-hole}\rangle$

make it difficult to directly compute  $Z_{\mathbf{k}_f}$  by using the definition (2). To overcome this difficulty, we note that a finite  $Z_{\mathbf{k}_f}$  implies a sudden jump in the momentum distribution function  $n(\mathbf{k}) \equiv \sum_{\sigma} \langle c_{\mathbf{k}\sigma}^{\dagger} c_{\mathbf{k}\sigma} \rangle$  at the Fermi momentum. Therefore, we first calculate  $n(\mathbf{k})$ , that is a task well within the reach of the DMRG method, and then proceed to find  $Z_{\mathbf{k}_f}$ . The results are shown in Fig. 3.

The insets of Fig. 3 present the hole momentum distribution  $1 - n(\mathbf{k})$  as a function of  $k_x$  for fixed  $k_y = 2\pi/3$  in the 3-leg ladder (a) and  $k_y = \pi/2$  in the 4-leg ladder (b). The value of  $k_y$  is chosen in the way that the ‘‘sudden change’’ in  $1 - n(\mathbf{k})$  can reach maxima by varying  $k_x$ , according to the contour plots in the  $k_x$ - $k_y$  plane (see Supplemental Information). It is very important that after the rescaling:  $1 - n(\mathbf{k}) \rightarrow [1 - n(\mathbf{k})]N$ , all the curves in the inset of Fig. 3(a) [or (b)] collapse into a universal curve shown in the corresponding main panel. If one defines the Fermi surface by the sudden jump in the momentum distribution function, then the two universal curves suggest that the quasiparticle weight  $Z_{\mathbf{k}_f}$  scales as  $1/N$  for large  $N$ , and vanishes in the thermodynamic limit.

To satisfy the sum rule,  $\sum_{\mathbf{k}} [1 - n(\mathbf{k})] = 1$ , the width of the jump in  $1 - n(\mathbf{k})$  must remain finite in the limit  $N \rightarrow \infty$ . This is clearly shown in Fig. 3, consistent with a finite localization length in the real space. Such a finite width in the momentum space may also look like a remnant Fermi pocket of the hole (cf. the contour plots in Supplementary Information), whose density is finite in the localization volume even in the limit  $N \rightarrow \infty$ . We have also calculated the momentum distribution of the hole at different ratios of  $t/J$ . As shown in Supplementary Information, for a given sample size, the jump near the Fermi point gets continuously reduced with increasing  $t/J$ , which is consistent with earlier work<sup>8</sup>.

Moreover, it has been predicted analytically<sup>15</sup> that a spin-charge separation occurs as a spinless holon is localized while a neutral spinon of  $S = 1/2$  moves away in the two-dimensional case. The present numerical simulations indeed confirm this prediction for the odd-leg ladders where the spin gap vanishes. Specifically, we inject a hole into a 3-leg ladder by removing a  $\downarrow$  spin electron. The results are shown in Fig.4: the hole (charge) is localized at the sample center whereas the extra spin of  $S^z = 1/2$  is spread along the  $x$  direction, with a (coarse grained) density  $\langle S_i^z \rangle_{c.g.}$  approximately uniform. (For the even-leg ladders, the spin gap renders the observation of the spin-charge separation more difficult. Indeed, it is required that the spin gap to be small enough, a condition that can be achieved only if the leg number is sufficiently large.)



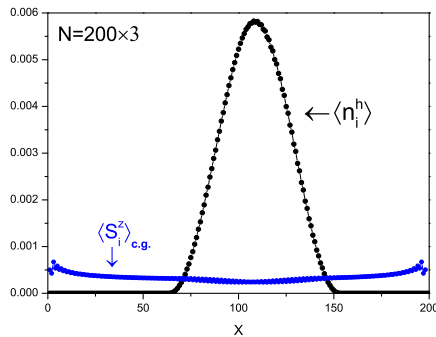


FIG. 4: **Spin-charge separation.** We remove a  $\downarrow$  spin electron in a  $N = 200 \times 3$  ladder and observe spin-charge separation. The hole (charge) is localized at the sample center, with the density distribution of Gaussian type; the spin of  $S^z = 1/2$  spreads over the entire sample, with the (coarse grained) density  $\langle S_i^z \rangle_{c.g.}$  approximately uniform. Note that to compute the spin density, a local coarse graining has been performed so as to average out local antiferromagnetic oscillations.

*Discussion.*— We note that in Fig. 1, the localization lengths are much larger than the lattice constant. This indicates that the injected hole moves “freely” from one site to the other within the localization volume. At larger (than the localization length) scales, such a free motion is fully suppressed, leading to the hole localization. In this sense, the scenario resembles the quasi-one-dimensional Anderson localization discovered by Efetov and Larkin long time ago<sup>25</sup>. There, quantum diffusion occurring at short scales is brought to a halt by wave interference at large scales. The phenomenological analogy notwithstanding, the two systems are fundamentally different: in the present system, there are no extrinsic disorders at all. Instead, as we will show below, the self-localization of the injected hole in the quantum antiferromagnetic background arises from intrinsic disorders of pure strong correlation origin. Therefore, it is distinctly different from either conventional Anderson localization<sup>17</sup> or many-body localization<sup>18</sup> discovered more recently.

Let us consider the motion of the hole in the quantum antiferromagnetic spin background from the injection point to a distant site (Fig. 5). The wave nature allows the hole to propagate along all the possible paths. As discovered in Refs. 13,14, given a hole path,  $p$ , the quantum phase is completely determined by the parity of the hole- $\downarrow$  spin exchange number,  $N_h^\downarrow[p]$ . More precisely, upon hopping to its nearest neighbor, the hole acquires

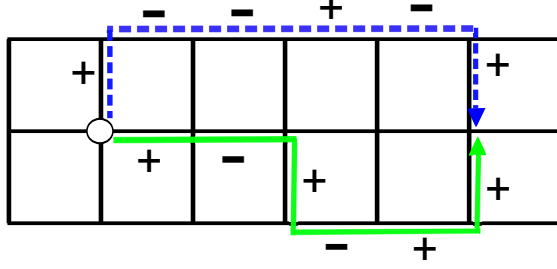


FIG. 5: **Interference picture of self-localization.** A sign  $\pm$  is acquired when the hole exchanges its position with the nearest neighbor, an  $\uparrow$  ( $\downarrow$ ) spin. Consequently, as the hole moves from the injection point to a distant site, a sign sequence – the phase string – is left behind as exemplified by the green (solid) and dashed (blue) lines. These phase strings destructively interfere with each other, suppressing the forward scattering and leading to the self-localization of the injected hole in the quantum antiferromagnetic spin background.

a sign,  $\pm$ , depending on whether it exchanges its position with  $\uparrow$  or  $\downarrow$  spin. As the hole moves along a given path, a sign sequence known as the phase string<sup>13,14</sup> is left behind. The quantum amplitude characterizing the hole motion is the superposition of all the propagation amplitudes associated with individual hole paths, and is given by

$$\sum_p \sum_{\{\phi\}} \rho_p[\{\phi\}] (-1)^{N_h^\downarrow[p]}, \quad (3)$$

where the first sum is over all the possible hole paths,  $p$ , the second over all the intermediate spin configurations,  $\{\phi\}$ , encountered in the path,  $p$ , and  $\rho_p[\{\phi\}] > 0$ . Equation (3) suggests that as a unique property of Mott physics, the spin configurations provide a translationally variant background – the analog of disorder potentials – for the hole motion.

To better understand the “disordering” nature of the phase strings, we note that as the hole path is slightly distorted, the intermediate spin configurations encountered may also be slightly changed. But the resulting change in the *parity* of the number  $N_h^\downarrow$  can be significant. That is, the “non-integrable quantum phase factor”,  $(-1)^{N_h^\downarrow[p]}$ , will strongly fluctuate as the hole paths are sampled. Then, from equation (3), we see that even paths close to each other can destructively interfere very singularly. As a result, the forward scattering is significantly suppressed, and eventually, localization is reached when the system is sufficiently large. Indeed, as the leg number or the parameter  $t/J$  increases, such destructive interference proliferates, resulting in the decrease of the localization length (Fig. 1 and 2).

In contrast, provided that the leg number is unity, the destructive interference from different paths no longer exists and the hole escapes from localization, in agreement with the numerical simulation (inset of Fig. 1). For the leg number comparable to the sample length, the destructive interference arising from the disordered signs leads to two-dimensional self-localization, as proved analytically in Ref. 15. Therefore, we conclude that the intrinsic “disordered” sign structure,  $(-1)^{N_h^\dagger[p]}$ , is responsible for the self-localization of the injected hole and the vanishing quasiparticle spectral weight.

In summary, we provide the first unambiguous numerical evidence showing that a single hole injected into Mott antiferromagnets is localized in the quantum antiferromagnetic background, and that the quasiparticle weight vanishes in the thermodynamic limit. These findings are consistent with both the analytic prediction of the phase string theory for a single hole-doped two-dimensional Mott antiferromagnet and the experimental results achieved by using ARPES and STM methods. In view of that the phase string effect is a rigorous property of the  $t$ - $J$  model on bipartite lattices regardless of doping concentration, temperature, and dimensions<sup>26</sup>, the present work may provide significant new insights into the long-standing issue of doped Mott insulators and thereby high temperature superconductivity.

This work was supported by the NNSFC (under grant nos. 10834003 and 11174174), by the KITP (NSF no. PHY05-51164), by the NSF MRSEC Program under Award (no. DMR 1121053), by the NBRPC (nos. 2009CB929402, 2010CB923003, 2011CBA00302 and 2011CBA00108), and by the Tsinghua University Initiative Scientific Research Program (no. 2011Z02151).

---

<sup>1</sup> P. W. Anderson, *The Theory of Superconductivity in the High-Tc Cuprate Superconductors* (Princeton University Press, Princeton, NJ, 1997).

<sup>2</sup> P. W. Anderson, *Physical Review Letters* **64**, 1839 (1990).

<sup>3</sup> B. I. Shraiman and E. D. Siggia, *Physical Review Letters* **61**, 467 (1988).

<sup>4</sup> S. Schmitt-Rink, C. M. Varma, and A. E. Ruckenstein, *Physical Review Letters* **60**, 2793 (1988).

<sup>5</sup> C. L. Kane, P. A. Lee, and N. Read, *Physical Review B* **39**, 6880 (1989).

<sup>6</sup> G. Martinez and P. Horsch, *Physical Review B* **44**, 317 (1991).

- <sup>7</sup> Z. Liu and E. Manousakis, *Physical Review B* **44**, 2414 (1991).
- <sup>8</sup> E. Dagotto, *Reviews of Modern Physics* **66**, 763 (1994).
- <sup>9</sup> P. W. Leung and R. J. Gooding, *Physical Review B* **52**, R15711 (1995).
- <sup>10</sup> T. K. Lee and C. T. Shih, *Physical Review B* **55**, 5983 (1997).
- <sup>11</sup> S. R. White and D. J. Scalapino, *Physical Review B* **55**, 6504 (1997).
- <sup>12</sup> R. B. Laughlin, *Physical Review Letters* **79**, 1726 (1997).
- <sup>13</sup> D. N. Sheng, Y. C. Chen, and Z. Y. Weng, *Physical Review Letters* **77**, 5102 (1996).
- <sup>14</sup> Z. Y. Weng, D. N. Sheng, Y.-C. Chen, and C. S. Ting, *Physical Review B* **55**, 3894 (1997).
- <sup>15</sup> Z. Y. Weng, V. N. Muthukumar, D. N. Sheng, and C. S. Ting, *Physical Review B* **63**, 075102 (2001).
- <sup>16</sup> C. Ye, P. Cai, R. Yu, X. Zhou, W. Ruan, Q. Liu, C. Jin, and Y. Wang (2012), 1201.0342.
- <sup>17</sup> P. W. Anderson, *Physical Review* **109**, 1492 (1958).
- <sup>18</sup> D. M. Basko, I. L. Aleiner, and B. L. Altshuler, *Annals of Physics* **321**, 1126 (2006).
- <sup>19</sup> P. W. Anderson, *Science (New York, N.Y.)* **235**, 1196 (1987).
- <sup>20</sup> P. A. Lee, N. Nagaosa, and X.-G. Wen, *Reviews of Modern Physics* **78**, 17 (2006).
- <sup>21</sup> B. O. Wells, Z.-X. Shen, A. Matsuura, D. M. King, M. A. Kastner, M. Greven, and R. J. Birgeneau, *Physical Review Letters* **74**, 964 (1995).
- <sup>22</sup> F. Ronning, C. Kim, D. L. Feng, D. S. Marshall, A. G. Loeser, L. L. Miller, J. Eckstein, I. Bozovic, and Z.-X. Shen, *Science* **282**, 2067 (1998).
- <sup>23</sup> K. M. Shen, F. Ronning, D. H. Lu, W. S. Lee, N. J. C. Ingle, W. Meevasana, F. Baumberger, A. Damascelli, N. P. Armitage, L. L. Miller, et al., *Physical Review Letters* **93**, 267002 (2004).
- <sup>24</sup> S. R. White, *Physical Review Letters* **69**, 2863 (1992).
- <sup>25</sup> K. B. Efetov and A. I. Larkin, *Sov. Phys. JETP* **58**, 444 (1983).
- <sup>26</sup> K. Wu, Z. Y. Weng, and J. Zaanen, *Physical Review B* **77**, 155102 (2008).

# SUPPLEMENTAL INFORMATION

## Self-localization of a single hole in Mott antiferromagnets

Zheng Zhu<sup>1</sup>, Hong-Chen Jiang<sup>2,3</sup>, Yang Qi<sup>1</sup>, Chu-Shun Tian<sup>1</sup> and Zheng-Yu Weng<sup>1</sup>

<sup>1</sup>*Institute for Advanced Study, Tsinghua University, Beijing, 100084, China*

<sup>2</sup>*Kavli Institute for Theoretical Physics, University of California,  
Santa Barbara, CA, 93106, U.S.A.*

<sup>3</sup>*Center for Quantum Information, IIS, Tsinghua University, Beijing, 100084, China*

(Dated: September 20, 2018)

At half-filling, the  $t$ - $J$  model reduces to the Heisenberg model. For the isotropic Heisenberg coupled-chain systems, the behavior of the even-leg ladders is dramatically different from that of the odd ones. A well-known fact is that the even-leg ladders have a spin gap, while the odd-leg ladders are gapless, leading to an exponential decay of the spin-spin correlation in the former, while a power law decay in the latter (see Fig. S1). The spin gap for the even-leg ladders is expected to vanish in the large leg number (namely two-dimensional) limit. The spin structure factor for the 4-leg case has already shown strong antiferromagnetic correlations as illustrated in Fig. S2. These results are consistent with earlier DMRG work<sup>1</sup>.

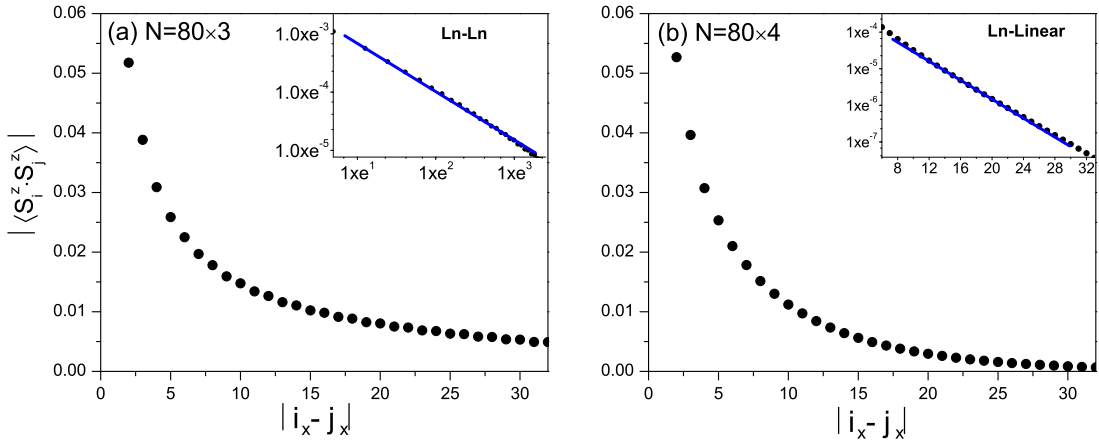


Fig. S1: The main panels show the spin-spin correlation  $|\langle S_i^z S_j^z \rangle|$  versus  $|i_x - j_x|$  with  $i_x$  and  $j_x$  located on the middle leg of 3-leg (a) and 4-leg ladder (b), respectively. The insets are ln-ln plot in (a) and ln-linear plot (b), fitted with the straight (blue) lines which indicate the power law decay for the former and exponential decay for the latter.

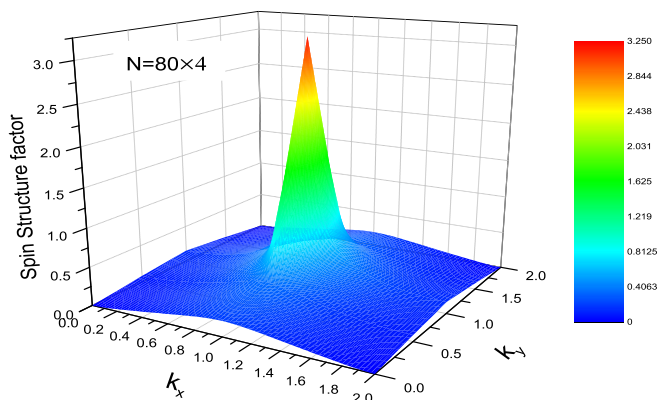


Fig. S2: Spin structure factor for the 4-leg ladder ( $N=80\times 4$ ), in which the peak is located at  $(\pi, \pi)$  indicating strong spin antiferromagnetic correlations even though a finite spin gap is present.

For the hole density distribution  $\langle n_i^h \rangle$  calculated in this work, the total hole number is fixed,  $\sum_i \langle n_i^h \rangle = 1$ . The contour plot  $\langle n_i^h \rangle$  in the  $x$ - $y$  plane of the ladder is illustrated in Fig. S3 for  $N = 40 \times N_y$  with  $N_y = 2, 3, 4$ , and 5. Besides the localization in the central region along the chain ( $x$ ) direction, a prominent feature in the profiles is the distinction between the even- and odd-leg ladders: the former has a spatial oscillation, while the latter has none. This is concomitant with the parity effect in the spin-spin correlation seen in Fig. S1.

Fig. S4 shows the contour plot of the electron momentum distribution function  $n(\mathbf{k})$  for the 3-leg (a) and 4-leg (b) cases, respectively at  $N_x = 80$ . The minimum of  $n(\mathbf{k})$  appears at  $k_y = \pm\pi/2$  for the 4-leg ladder and  $k_y = \pm 2\pi/3$  for the 3-leg ladder. The jump of the hole momentum distribution as a function of the ratio  $t/J$  is shown in Fig. S5, which indicates that the jump is monotonically reduced with the increase of  $t/J$ .

---

<sup>1</sup> S.R.White, R. M. Noack, and D. J. Scalapino. Phys. Rev. Lett. **73**, 886(1994).

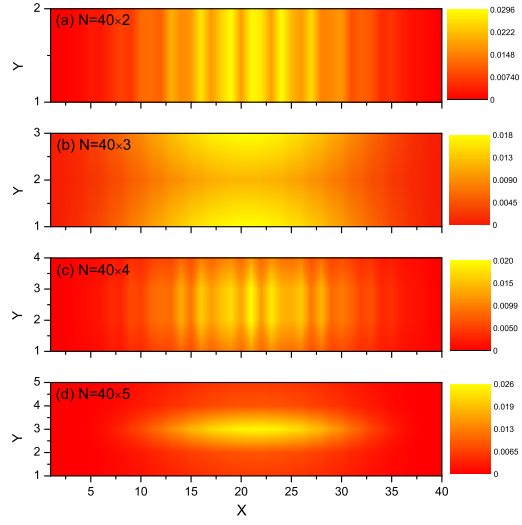


Fig. S3: Contour plots of the hole distribution in real space. The sample size  $N$  is  $40 \times 2$  (a),  $40 \times 3$  (b),  $40 \times 4$  (c), and  $40 \times 5$  (d) from top down.

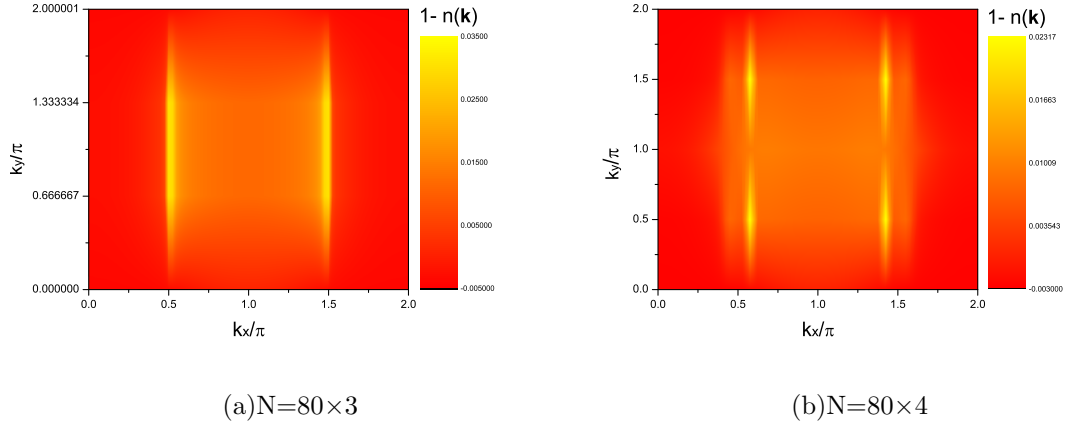


Fig. S4: Contour plots of the electron momentum distribution  $n(\mathbf{k})$  for 3-leg (a) and 4-leg (b) ladders.

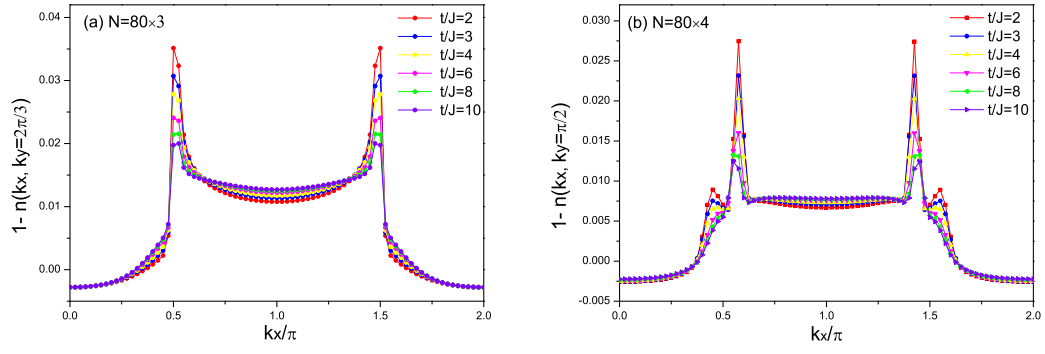


Fig. S5: The hole momentum distribution at different ratios of  $t/J$  for 3-leg (a) and 4-leg (b) ladders.